Physica Scripta. Vol. T32, 122–125, 1990.

Deconfinement Signature, Mass Dependence of Transverse Flow and Time Evolution in Antiproton–Proton Collisions at $\sqrt{s} = 1.8\,\text{TeV}$

T. Alexopoulos,[6] C. Allen,[5] E. W. Anderson,[3] H. Areti,[2] S. Banerjee,[4] P. D. Beery,[4] N. N. Biswas,[4] A. Bujak,[5] D. D. Carmony,[5] T. Carter,[1] P. Cole,[5] Y. Choi,[5] R. De Bonte,[5] A. Erwin,[6] C. Findeisen,[6] A. T. Goshaw,[1] L. J. Gutay,[5] A. S. Hirsch,[5] C. Hojvat,[2] V. P. Kenney,[4] C. S. Lindsey,[3] J. M. LoSecco,[4] T. McMahon,[5] A. P. McManus,[4] N. Morgan,[5] K. Nelson,[6] S. H. Oh,[1] J. Piekarz,[4] N. T. Porile,[5] D. Reeves,[2] R. P. Scharenberg,[5] S. R. Stampke,[4] B. C. Stringfellow,[5] M. Thompson,[6] F. Turkot,[2] W. D. Walker,[1] C. H. Wang,[3] and D. K. Wesson,[1]

[1]Department of Physics, Duke University, Durham, North Carolina 27706, U.S.A.
[2]Fermi National Accelerator Laboratory, Batavia, Illinois 60510, U.S.A.
[3]Department of Physics, Iowa State University, Ames, Iowa 50011, U.S.A.
[4]Department of Physics, University of Notre Dame, Notre Dame, Indiana 46556, U.S.A.
[5]Department of Physics and Chemistry, Purdue University, West Lafayette, Indiana 47907, U.S.A.
[6]Department of Physics, University of Wisconsin, Madison, Wisconsin 53706, U.S.A.

Received January 2, 1990; accepted February 1, 1990

Abstract

The yields and the transverse momentum distributions of pions, kaons, and antiprotons produced in the central region of $\bar{p}p$ collisions at $\sqrt{s} = 1.8\,\text{TeV}$ at the Fermilab Tevatron collider have been measured up to a charged particle pseudo-rapidity density of approximately 20. The average transverse momentum $\langle p_t \rangle$ as a function of $\langle dN_c/d\eta \rangle$ for all three types of particles is presented. We find that transverse flow does not explain the $\langle p_t \rangle$ separation. The most plausible interpretation is that the $\langle p_t \rangle$ vs. N_c spectra represent in isobar in the two phase region.

Particle production data in high energy hadron–hadron collisions over a broad range of transverse momenta are important for testing the validity of any strong interaction theory. The study of particle production as a function of multiplicity, or energy density, is also relevant to recent speculation as to a possible phase transition of hadronic matter to a deconfined quark–gluon state [1]. In this letter we report results on the production of mass-identified $\pi^{\pm}$, $K^{\pm}$ and $\bar{p}$ at a CMS energy $\sqrt{s} = 1.8\,\text{TeV}$, for transverse momentum $0.2 < p_t < 1.5\,\text{GeV}/c$, and charged multiplicity $15 < N_c < 130$. The data come from a sample of $-400\,000$ charged hadrons that are mass identified by a spectrometer system with time-of-flight (TOF) in an experiment at the C0 intersection during the first run of the Fermilab $p\bar{p}$ collider. Using the same data, the dependence of $\langle p_t \rangle$ on N_c for undifferentiated hadron production has been reported previously [2].

The detector for this experiment includes a 240-counter multiplicity hadoscope surrounding the collision region, a magnetic spectrometer at polar angle $\theta = 90°$, and a TOF system. Details of the multiplicity hadoscope, with coverage $-3.25 \leqslant \eta \leqslant +3.25$ in pseudorapidity, and the magnetic spectrometer, with acceptance $-0.36 \leqslant \eta \leqslant +1.0$ and $0° \leqslant \phi \leqslant 20°$ in azimuth, have been give previously [2]. We measure the charged multiplicity N_c and the mean multiplicity density $\langle dN_c/d\eta \rangle$, over the fixed pseudorapidity interval of the hodoscope. The rapidity (y) acceptance of the spectrometer is mass and momentum dependent, and is calculated on a track by track basis.

The design and performance of the TOF system have been reported in a NIM article [3]. The present experiment uses two 9-counter hodoscopes surrounding the Tevatron beam pipe $\pm 2\,\text{m}$ from the nominal interaction point to generate a t_0 signal when at least one fast forward particle from a beam–beam interaction is seen in each hodoscope. In the spectrometer arm, TOF arrays are placed at 2 m (TOF1) and 4 m (TOF2) from the interaction point. These two TOF arrays play complementary roles in π–K separation: the 2 m TOF1 is more effective in the analysis of low-momentum kaons which decay before reaching the 4 m TOF2, while the 4 m TOF2 is more effective in resolving high-momentum K's and π's. Mass distributions show clear $\pi^{\pm}$, $K^{\pm}$ and $p/\bar{p}$ peaks [3] allowing $K^{\pm}$ ($p^{\pm}$) identification for momentum $p \leqslant 1.1$ (1.4) GeV/c at 2 m and $p \leqslant 1.5$ (1.8) GeV/c at 4 m. An $e^{\pm}$ peak is visible below 0.2 GeV/c with an amplitude falling steeply with p, as expected from π^0 decay effects. These data in conjuction with a simulation of $e^{\pm}$ production indicate that the $e^{\pm}$ background to the π's is less than 5% in the data reported. The TOF system resolution, as estimated from mass-squared peaks widths averaged over the entire run, is 140 ps, slightly higher than the $\sigma = 110\,\text{ps}$ achieved [3] over short periods immediately following laser calibration runs. From Monte Carlo fits we select $-0.14 < M^2 < 0.16\,\text{GeV}^2$ as the pion mass region, $0.16 \leqslant M^2 \leqslant 0.36\,\text{GeV}^2$ as the $K^{\pm}$ mass region and $0.5 \leqslant M^2 \leqslant 1.4\,\text{GeV}^2$ as the mass region for $p/\bar{p}$. Positive and negative pion and kaon data agree and have been combined. There is an excess of p over $\bar{p}$ at low momentum, (the $p/\bar{p}$ ratio ≈ 2 for $0.3 \leqslant p \leqslant 0.6\,\text{GeV}/c$), consistent with the higher bakground of secondary protons expected from the interactions of pions with the surrounding beam pipe. We therefore present data on produced $\bar{p}$'s only.

All data are corrected for mass identification efficiency, decay, and geometrical acceptance. The correction factors are determined via a Monte Carlo calculation by generating particles of various momenta and passing them through the spectrometer arm. Hit patterns in the tracking chambers are simulated, including decays and secondary interactions; these patterns are then used to reconstruct tracks through the

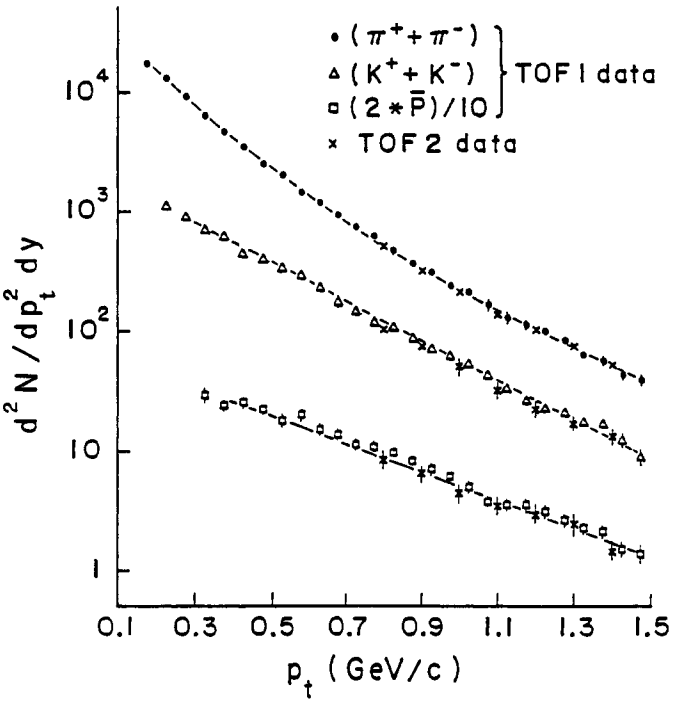

Fig. 1. Plot of inclusive d^2N/dp_t^2dy as a function of p_t for pions, kaons and antiprotons. The particles are mass-identified using two independent hodoscopes, TOF1 and TOF2 (see text) and the results from both detectors are shown as a consistency check. The curves shown correspond to fits (described in the text) in the regions, $0.2 < p_t < 1.5\,\text{GeV}/c$ (pions), $0.25 < p_t < 1.5\,\text{GeV}/c$ (kaons), and $0.35 < p_t < 1.5\,\text{GeV}/c$ (antiprotons).

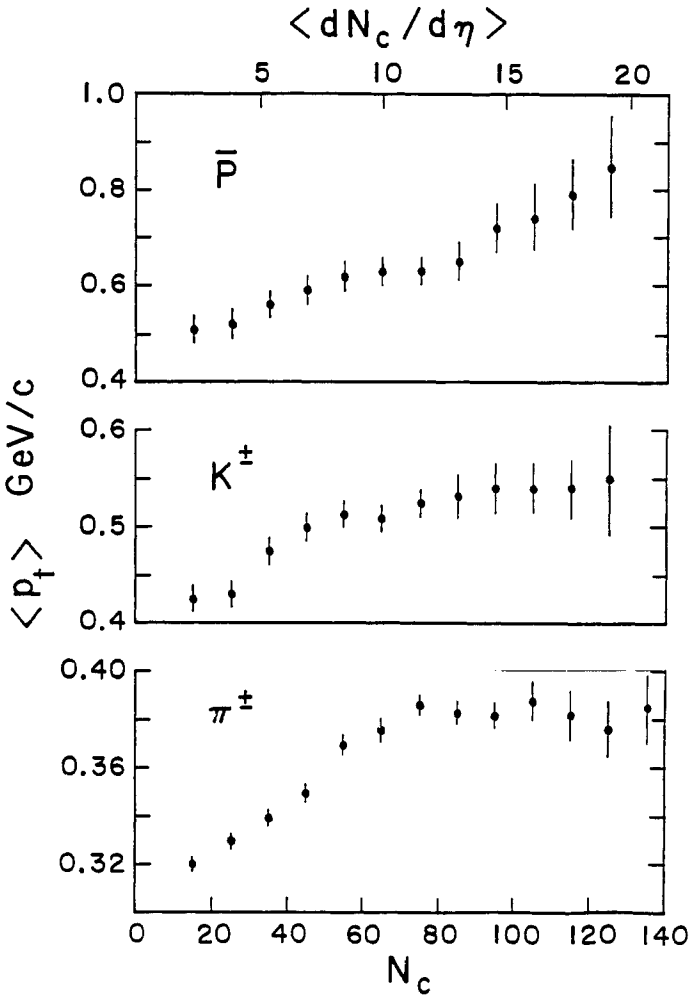

Fig. 2. (a)–(c) Plots of $\langle p_t \rangle$ vs $dN_c/d\eta$ (or N_c) for $\bar{p}$, kaons and pions respectively, for particle with $p_t < 1.5\,\text{GeV}/c$.

magnet, to ascertain momenta, and to obtain the expected times of flight, which are then smeared using the experimentally determined time resolution. The efficiency is then calculated as the ratio of the number of Monte Carlo events fulfilling the selection criteria used in the data to the total number of generated events. The efficiency matrix depends on six variables; charge, mass, vertex position, momentum, polar angle θ, and N_c. These correction factors are used event-by-event.

Figure 1 shows the invariant distribution d^2N/dp_t^2dy, averaged over y, for mass-identified pions, kaons and antiprotons in minimum bias events. Here each track is weighted by $(\Delta y)^{-1}$, where Δy is the difference between the upper and lower values of rapidity accepted by the spectrometer arm; these rapidity limits depend on charge, mass, p_t, and vertex position and are determined by the Monte Carlo calculation. The lower p_t cutoff values of 0.20, 0.25 and 0.35 GeV/c for pions, kaons and antiprotons respectively are dictated by considerations of track curvature in the magnetic field, decay, dE/dx losses and backgrounds.

The kaon and antiproton data have been fitted with exponentials of the form $dN/dp_t^2 \propto \exp(-\alpha p_t)$ in the regions $0.25 < p_t < 1.5\,\text{GeV}/c$ for kaons, and $0.35 < p_t < 1.5\,\text{GeV}/c$ for antiprotons, where $\alpha = 3.69 \pm 0.05\,(\text{GeV}/c)^{-1}$ for kaons and $\alpha = 2.80 \pm 0.07\,(\text{GeV}/c)^{-1}$ for antiprotons. The pion data for $0.15 < p_t < 1.5\,\text{GeV}/c$, can be parameterized with a power law [4], $dN/dp_t^2 \propto (p_t + p_0)^{-n}$ yielding $n = 8.13 \pm 0.04$ with $p_0 = 1.0\,\text{GeV}/c$ (fixed). The curves shown in Fig. 1 correspond to these parameters. Using these fitted values, we compute the number of particles and the average transverse momentum for $0.0 < p_t < 1.5\,\text{GeV}/c$. The $\langle p_t \rangle$ values for pions, kaons and $\bar{p}$ are 0.362 ± 0.003, 0.51 ± 0.01 and $0.61 \pm 0.02\,\text{GeV}/c$ respectively [5]. The K/π and $\bar{p}/\pi$ ratios are 0.112 ± 0.004 and 0.074 ± 0.006 in equal regions of central rapidity.

Values of average transverse momentum $\langle p_t \rangle$ are presented in Fig. 2 as a function of charge multiplicity N_c, obtained from the number of hits in the multiplicity hodoscope [2]. The average pseudorapidity density, $\langle dN_c/d\eta \rangle$, is obtained by dividing N_c by 6.5, the pseudorapidity acceptance of the multiplicity hodoscope. Explanations for the rise in $\langle p_t \rangle$ with increasing N_c (or $\langle dN_c/d\eta \rangle$) and the apparent plateau observed at higher N_c values have been offered by several authors [1, 6]. We simply note here that the features of the correlation between $\langle p_t \rangle$ and $\langle dN_c/d\eta \rangle$ observed for undifferentiated hadron production in our previous paper [2] seem to be present for $\bar{p}$, K and π production separately in the mass-identified data. The "plateau" region $8 \leqslant \langle dN_c/d\eta \rangle \leqslant 15$ corresponds [7] to an energy density $\varepsilon_0 = 1.5$–$3.0\,\text{GeV/fm}^3$ for hadronic matter, assuming average transverse energy to be $= 0.4\,\text{GeV}$ (pions).

Ratios of K/π and $\bar{p}/\pi^-$ of production cross sections averaged over the central region are shown as a function of charged multiplicity N_c in Fig. 3 and as a function of p_t in Fig. 4. In Fig. 3 the K/π ratio appears to increase with multiplicity, reaching a value $K/\pi = 0.14$. The ratio $\bar{p}/\pi^-$ is, by contrast, quite constant, consistent with the average value of 0.074 over the entire range of multiplicity. Corrections for systematic errors in computing background subtractions, particle decays and interactions, mass identification, and

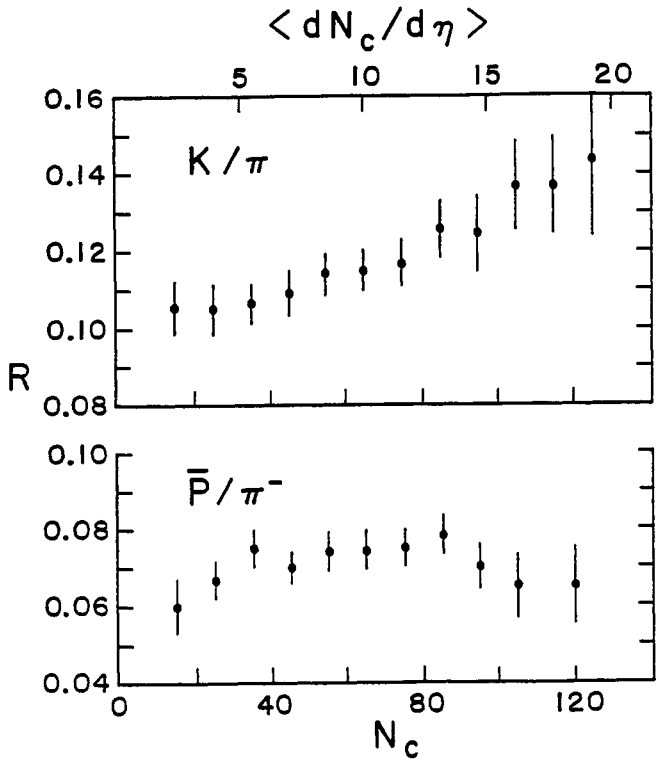

Fig. 3. Ratios of K/π and $\bar{p}/\pi^-$ as a function of charged multiplicity N_c. The ratios are calculated for equivalent rapidity intervals.

geometrical acceptance have not been made in the data shown. Studies [8] indicate that the systematic error in $\langle p_t \rangle$ is of the order of 6% at low N_c and 10% at high N_c. The systematic error in K/π and $\bar{p}/\pi$ varies from 10–15%.

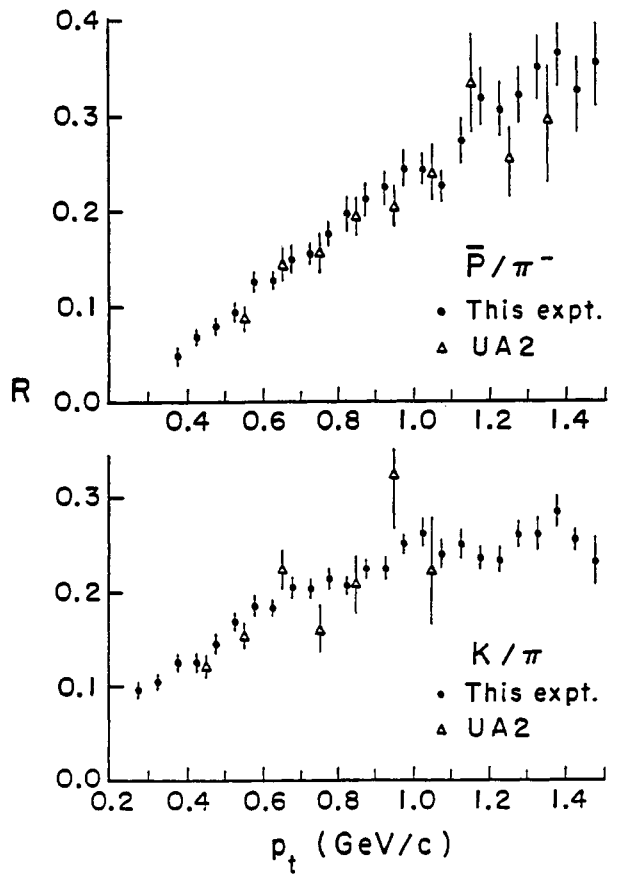

Fig. 4. (a)–(b) Ratios of K/π and $\bar{p}/\pi^-$ as a function of p_t from this experiment, compared with UA2 data at $\sqrt{s} = 546$ GeV.

Table I. $\langle p_t \rangle$ *and* K/π *as a function of* $\sqrt{s}$

$\sqrt{s}$ GeV	$\langle p_t \rangle$ GeV/c	K/π
UA5 200	0.47 ± 0.07	0.089 ± 0.011
546	0.49 ± 0.03	0.095 ± 0.009
900	0.51 ± 0.07	0.100 ± 0.008
E735 1800	0.51 ± 0.01	0.112 ± 0.004

The ratio of $\bar{p}/\pi^-$ rises with transverse momentum p_t, Fig. 4, up to a value of ~ 0.35 for $p_t > 1.2$ GeV/c. The K/π ratio rises less steeply and appears to level off at a value of ~ 0.25 for all $p_t > 0.9$ GeV/c. Corresponding data from the CERN UA2 experiment [9] at $\sqrt{s} = 546$ GeV, plotted for comparison, show similar trends.

The CERN UA5 group [10] has studied neutral kaon production at $\sqrt{s} = 200$, 546 and 900 GeV, and it is possible to compare their $\langle p_t \rangle$ values and K/π ratios with data on charged kaons from the present 1800 GeV experiment (Table I). The values of $\langle p_t \rangle$ for neutral kaons for $0.0 < p_t < 1.5$ GeV/c are calculated at 200, 546 and 900 GeV using UA5's own fitting parameters. The results of Table I suggest that there is no significant change in Kaon $\langle p_t \rangle$ with CMS energy.

The UA5 ratios of K/π at $\sqrt{s} = 200$, 546 and 900 GeV and our value at 1800 GeV are also shown in Table I. The data show a slow increase of K/π with CMS energy.

In Figs. 5, 6 and 7 we present the $d^2N/dp_t^2 dy$ distribution

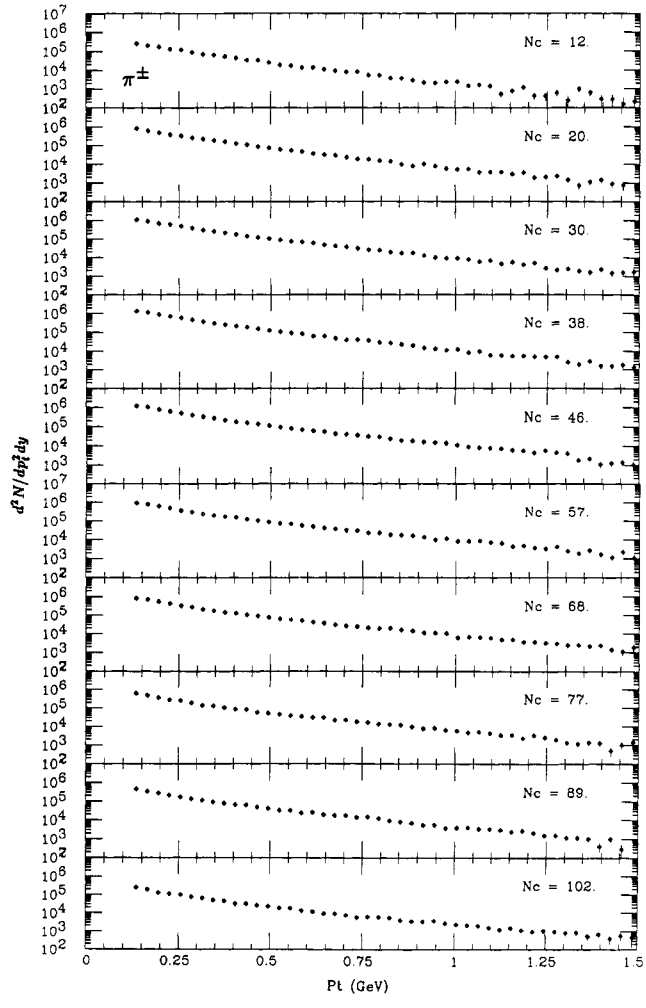

Fig. 5. Plot of inclusive $d^2N/dp_t^2 dy$ as a function of p_t for pions in intervals of multiplicity N_c.

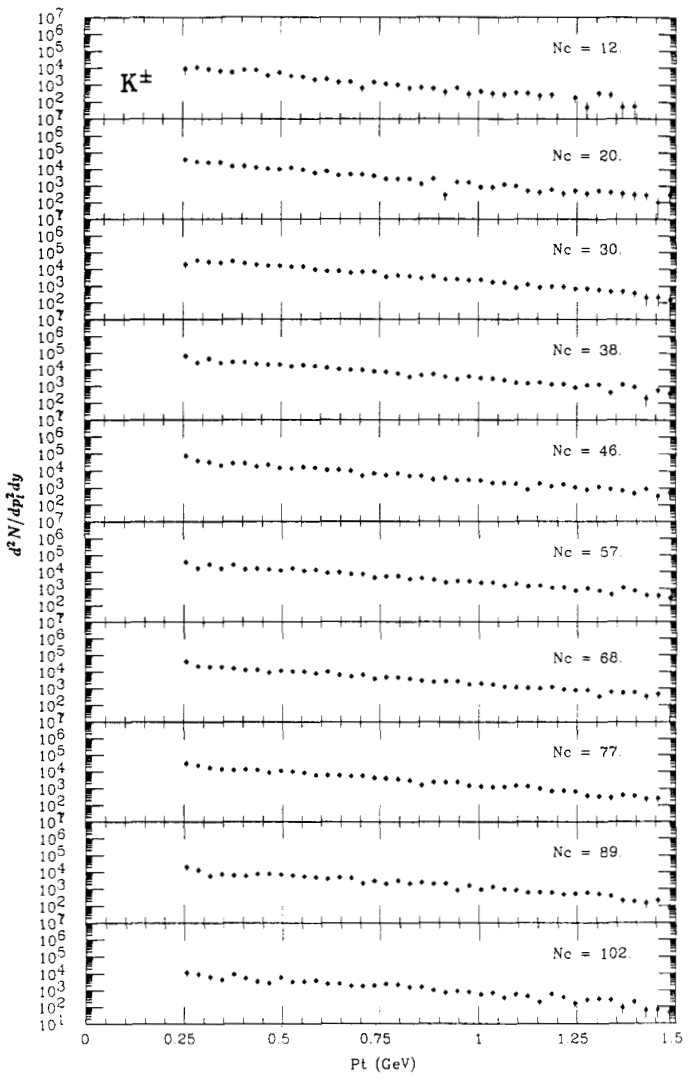

Fig. 6. Plot of inclusive d^2N/dp_t^2dy as a function of p_t kaons in intervals of multiplicity N_c.

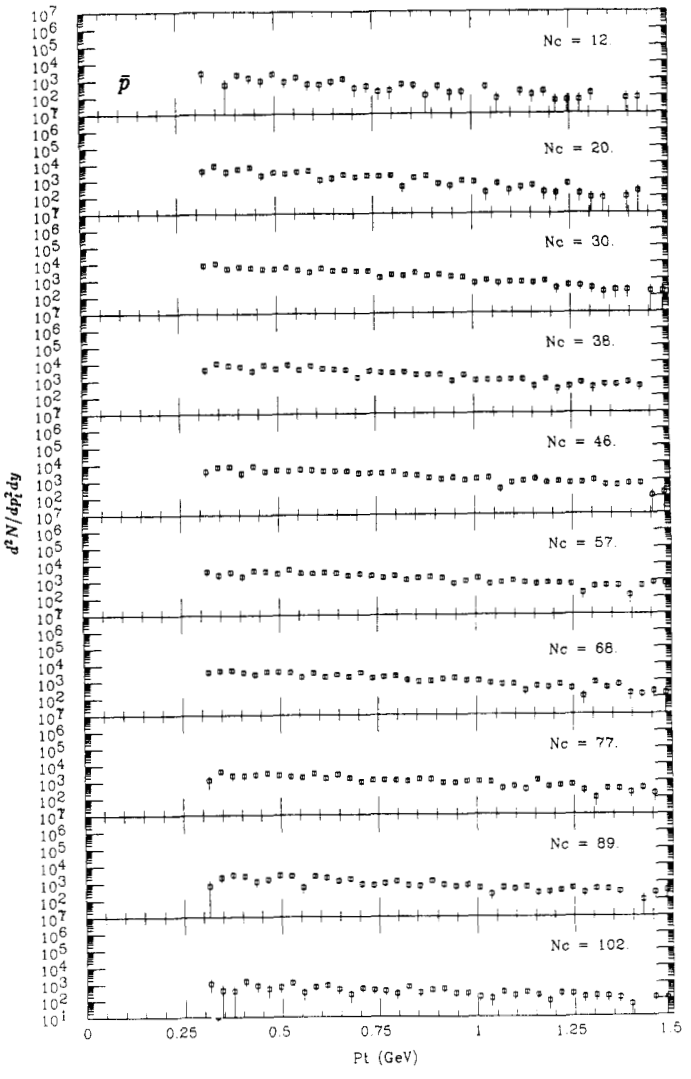

Fig. 7. Plot of inclusive d^2N/dp_t^2dy as a function of p_t for antiprotons in intervals of multiplicity N_c.

for π, K and $\bar{p}$ from which the $\langle p_t \rangle$ were obtained. Preliminary fits with the Barz–Csernai transverse flow model give a reasonably good fit but do not explain the large difference in $\langle p_t \rangle$ for π, K and $\bar{p}$. Thus the speaker interprets these results as follows: The $\langle p_t \rangle$ vs N_c are T vs S isobar curves, consistent with a first order phase transition, where the third thermodynamic variable the pressure is fixed for a given mass. Superimposed on this thermal picture is the radial flow which transforms the exponential fall off of the p_t distribution of the pions into a power law.

References

1. Van Hove, L., Phys. Lett. **118B**, 138 (1982); McLerran, L. D. and Svetitsky, B., Phys. Lett. **98B**, 195 (1981); Kuti, J., Polonyi, J. and Szlachanyi, K., Phys. Lett. **98B**, 199 (1981); Kogut, J. *et al.*, Phys. Rev. Lett. **51**, 869 (1983).
2. Alexopoulos, T., *et al.*, Phys. Rev. Lett. **60**, 1622 (1988).
3. Banerjee, S., *et al.*, Nucl. Inst. Meth. **A269**, 121 (1988).
4. Arnison, G., *et al.*, Phys. Lett. **118B**, 167 (1982); Abe, F., *et al.*, Phys. Rev. Lett. **61**, 1819 (1988).
5. Errors stated are statistical. If in place of the functions mentioned we extrapolate to $p_t = 0$ by using $\exp(-\sqrt{m^2+p_t^2}/B)$ matched to the slop and magnitude at the lowest observed p_t, then the $\langle p_t \rangle$ values become 0.372, 0.560 and 0.638 for π, K and $\bar{p}$ respectively. Systematic errors from other sources are estimated to be less than 7%.
6. Bkorken, J. D., Phys. Rev. **D27**, 140 (1983).
7. We used 1 fm for the radius and the lifetime in expressions given in Ref. [6], where we have multiplied by 2 to corrent the expression for ε_0.
8. To be reported elsewhere. We also note that the production of unstable particles whose flight paths are comparable to the vertex resolution (5 cm) of our system can make finite contributions to the p_t spectra shown. For example, a simple estimate indicates that K_s^0 production may contribute about 8% of the $\pi^\pm$ curve at low p_t.
9. Banner, M., *et al.*, Phys. Lett. **122B**, 322 (1983); Banner, M., *et al.*, Z. Phys. **C27**, 329 (1985).
10. Alpgard, K., *et al.*, Phys. Lett. **115B**, 65 (1982); Ansorge, R. E., *et al.*, Z. Phys. **C41**, 179 (1988) (and references cited therein).